



# Role of contrast-enhanced magnetic resonance high-resolution variable flip angle turbo-spin-echo (T1 SPACE) technique in diagnosis of transverse sinus stenosis

Tao Quan<sup>a</sup>, Yanan Ren<sup>b</sup>, Yanan Lin<sup>b</sup>, Sheng Guan<sup>a</sup>, Haiman Hou<sup>c</sup>, Baojun Yan<sup>a</sup>,  
Jingliang Cheng<sup>b,\*</sup>, Haowen Xu<sup>a,\*</sup>

<sup>a</sup> Department of Interventional Neuroradiology, the First Affiliated Hospital of Zhengzhou University, 1st of Jianshe Road, Zhengzhou, Henan, China

<sup>b</sup> Department of Magnetic Resonance, the First Affiliated Hospital of Zhengzhou University, 1st of Jianshe Road, Zhengzhou, Henan, China

<sup>c</sup> Department of Neurology, the First Affiliated Hospital of Zhengzhou University, 1st of Jianshe Road, Zhengzhou, Henan, China

## ARTICLE INFO

### Keywords:

Digital subtraction angiography  
Idiopathic intracranial hypertension  
Magnetic resonance imaging  
Cranial sinuses

## ABSTRACT

**Purpose:** Transverse sinus stenosis (TSS) is the most sensitive imaging characteristic of idiopathic intracranial hypertension (IIH). This study aimed to assess the diagnostic performance of contrast-enhanced magnetic resonance high-resolution variable flip angle turbo-spin-echo (T1 SPACE) technique in TSS patients and evaluate the diagnostic accuracy of enhanced T1 SPACE, and phase-contrast magnetic resonance venography (PC MRV) with digital subtraction angiography (DSA) as standard imaging.

**Method:** This prospective study enrolled 62 patients with suspected IIH and PC MRV-confirmed transverse sinus stenosis. All patients underwent lumbar puncture, PC MRV, enhanced T1 SPACE sequences and DSA examination. The accuracy, sensitivity, and specificity of enhanced T1 SPACE in detecting venous sinus stenosis were calculated and compared with those of PC MRV. Intermodality agreement (Kendall's rank correlation coefficients and weighted kappa statistic) was assessed.

**Results:** Sixty-two patients were enrolled from November 2016 to October 2018. For the measured stenosis, better correlation was observed in enhanced T1 SPACE and DSA (AUC = 0.953) than PC MRV (AUC = 0.871). Intermodality agreement of enhanced T1 SPACE ( $r_k = 0.895$  and weighted  $\kappa = 0.868$ ) was better than PC MRV ( $r_k = 0.753$  and weighted  $\kappa = 0.653$ ) compared with DSA. Thirty-seven intrasinus filling defects were detected by contrast-enhanced T1 SPACE, while only twenty of them were detected on source imaging of PC MRV.

**Conclusions:** The contrast-enhanced T1 SPACE sequence was more sensitive and specific compared with PC MRV in assessing stenosis and detecting lesions in TSS patients. Accurate determination of the presence and extent of TSS using this technique might be useful in patient selection and guiding the treatment.

## 1. Introduction

Transverse sinus stenosis (TSS) has been regarded as the most sensitive imaging characteristic of idiopathic intracranial hypertension (IIH) [1–4]. Epidemiological studies have estimated that the prevalence of TSS in patients with IIH ranges from 50% to 90% [5–7]. An early imaging examination might be useful in choosing optimal medical therapy or early invasive management. Digital subtraction angiography (DSA) is the “gold standard” for diagnosing and characterizing intracerebral sinus stenosis [8]. However, DSA is invasive and may lead to complications associated with the procedure. Various specific magnetic

resonance imaging (MRI) techniques are available for evaluating suspected abnormalities of the transverse sinuses [3,9–11]. The phase-contrast (PC) MRV has been widely used to detect the stenosis of transverse sinus in patients with IIH patients. A major pitfall of PC MRV is the artifactual intravascular signal loss that occurs at predictable points in the intracranial venous anatomy, namely, the posterior superior transverse sinus, transverse–sigmoid junction, and sigmoid sinuses [9,10]. However, the chronic, partially recanalized venous sinus thrombosis might be misdiagnosed as sinus wall for their similar signals on PC MRV sequence. Some patients with chronic sinus thrombosis may be misdiagnosed as IIH and received inappropriate therapy with an

**Abbreviations:** AUC, area under the curve; T1 SPACE, high-resolution variable flip angle turbo-spin-echo; CNR, carrier noise ratio; TSS, transverse sinus stenosis; ICP, intracranial pressure; IIH, idiopathic intracranial hypertension; SD, standard deviation

\* Corresponding authors.

E-mail addresses: [cjr.chjl@vip.163.com](mailto:cjr.chjl@vip.163.com) (J. Cheng), [neuron@126.com](mailto:neuron@126.com) (H. Xu).

<https://doi.org/10.1016/j.ejrad.2019.108644>

Received 16 March 2019; Received in revised form 16 July 2019; Accepted 28 August 2019

0720-048X/© 2019 Elsevier B.V. All rights reserved.

unfavorable clinical outcome [12]. In this regard, the accuracy of PC MRV has been questioned [13,14].

T1 SPACE imaging was developed for the detection and evaluation of brain or meningeal metastasis as it suppresses normal blood vessel signals in the brain surface [15]. This technique received wide interests because it can isolate the thrombus from surrounding tissues, including lumen and wall, to achieve accurate and early detection of the thrombus in the cerebral venous system. The use of black-blood thrombus imaging may improve the accuracy of subacute venous sinus thrombosis diagnosis [16,17], and it might be an effective way to identify chronic thrombus and hyperplasia of sinus wall. However, the sensitivity and specificity of this technique in detecting transverse sinus stenosis are still unknown.

The present study was performed to assess the diagnostic performance of contrast-enhanced T1 SPACE in patients with TSS and evaluate the diagnostic accuracy and inter-observer variability of enhanced T1 SPACE, PC MRV compared with DSA as standard imaging.

## 2. Materials and methods

### 2.1. Study population

This study was approved by the institutional review board, and written informed consent was obtained from all patients.

From November 2016 to October 2018, 62 patients with suspected IIH and PC MRV-confirmed transverse sinus stenosis were prospectively enrolled in the study. Inclusion criteria for the study are as follows: (1) age  $\geq$  18 years; (2) patients admitted to hospital had headache, visual loss, or tinnitus; (3) transverse sinus stenosis were confirmed by PC MRV after admission. The exclusion criteria were as follows: (1) the duration of clinical symptoms was less than 1 month; (2) hydrocephalus, intracranial mass, or structural lesion; (3) primary ocular or aural disease; (4) abnormal coagulation; (5) and abnormal cerebrospinal fluid composition. All enrolled patients underwent lumbar puncture, PC MRV, and enhanced T1 SPACE before DSA examination. The lumbar puncture was performed 2–4 days (mean, 3 days) before MR sequences. Only a few milliliters of cerebrospinal fluid (CSF) were collected for cytological and biochemical examination. The interval between two MR sequences ranged from 0 to 2 days (mean, 1 days), and the interval between MR sequences and DSA studies ranged from 1 to 4 days (mean, 2 days).

### 2.2. MR techniques

MR examinations were performed using a 3.0-T MR scanner (Prisma; Siemens Healthcare, Germany) with a 32-channel head coil for signal reception. The parameters of the 3D-PC-MRV sequence, enhanced T1 SPACE sequence are summarized in Supplement Table 1. The enhanced T1 SPACE images were obtained with the following parameters: repetition time = 650 ms; echo time = 13 ms; matrix size = 320; field of view = 260 mm; slice thickness = 0.7 mm; acquisition time = 5 min 27 s).

### 2.3. DSA technique

Patients underwent cerebral angiography examinations on a fixed digital angiographic system with a single-plane flat panel detector (FD 20 Artis; Phillips Medical Systems, France). All procedures were performed with local anesthesia and/or conscious sedation. Blood pressure, and electrocardiogram saturation values were monitored during the procedure. Femoral arterial access was used in all cases. Contrast media (Omnipaque 300; GE Healthcare) was injected intra-arterially over the sheath using a power injector. After a 5-Fr catheter was selectively placed in the internal carotid artery, 8 mL contrast media was injected at a flow rate of 4 mL/s through the catheter. Imaging of cerebral venous sinuses was performed in both frontal and lateral positions

**Table 1**  
Baseline characteristics of the study population.

	n/N (%)
<b>Demographics</b>	
Mean age, year (SD)	37.8 $\pm$ 13.3
Sex (% of women)	45/62 (72.48%)
<b>Clinical characteristics</b>	
Headache	38/62 (61.3%)
Papilledema	21/62 (33.9%)
Focal neurological deficit	3/62 (4.8%)
Mean BMI, kg/m <sup>2</sup> (SD)	25.77 $\pm$ 3.48 kg/m <sup>2</sup>
Mean CSF opening pressure, mmH <sub>2</sub> O (SD)	311 $\pm$ 113 mmH <sub>2</sub> O
<b>MR characteristics</b>	
Intrasinus filling defects	25/62 (40.3%)
Empty sella	17/62 (27.4%)
Posterior globe flattening	7/62 (11.3%)
Vertical tortuosity of the optic nerve	17/62 (27.4%)

BMI: body mass index; CSF: cerebrospinal fluid.

per side. In some cases, magnification, oblique, or high-frame-rate angiography was used when appropriate. If intrasinus lesions were confirmed by arteriography, femoral venous access was also used, and selected venous pressure measurement was performed. After examination, the catheter was removed, and hemostasis at the groin was achieved with manual compression.

### 2.4. Image evaluation

The right and left sides of the transverse-sigmoid sinus were evaluated separately. The number of transverse-sigmoid sinuses in 62 patients was 124 segments. The grade scale for each transverse-sigmoid conduit was determined separately, defined by the highest degree of stenosis encountered from the torcula to the jugular vein, and given a corresponding number from 0 to 4: 0 = discontinuity (gap) or aplastic segment; 1 = hypoplasia or severe stenosis within a segment of the conduit estimated as less than 25% of the cross-sectional diameter of the lumen of the distal superior sagittal sinus; 2 = moderately stenosed segment of the conduit (25%–50%); 3 = mildly narrowed segment (50%–75%); and 4 = no significant narrowing seen (75%–100%) [6].

MR images were interpreted independently by two radiologists who had an experience in MR angiography for 4 and 6 years, respectively. They were blinded to patient data and the results of DSA. PC MRV and enhanced T1 SPACE imaging were evaluated within different reading sessions.

The imaging analysis was performed on a picture archiving and communication system. The source data of vein-sinus cavity, morphology of sinus wall-, location of stenosis (peripheral or central), location of lesions (intra- or extrasinus), and other characteristic neuroimaging features of IIH, including empty sella, posterior globe flattening, and vertical tortuosity of the optic nerve were recorded [18,19]. The readers assessed venous sinus visualization, grading of stenosis or occlusion, arterial contamination, and diagnostic utility according to the aforementioned categories. Inconsistent individual assessments were re-evaluated and debated by two readers until a consensus was reached. The DSA images were analyzed by an experienced neurointerventional professor independently. After the blinded study, the observers, by consensus, looked for the reason for any incorrect interpretations on MR sequences using DSA imaging as the reference standard.

### 2.5. Statistical analysis

Quantitative variables were described as mean  $\pm$  standard deviation (SD); percentages were reported for categorical variables. The statistical measures of performance of the MR techniques and the specific signs were calculated using DSA as the reference standard. On the

basis of cross-tabulations, the sensitivity, specificity, and area under the curve (AUC) of different MR imaging findings were calculated (95% confidence interval, CI). Weighted kappa statistics were used to estimate inter-observer agreement with regard to TSS. The relationship among PC MRV, enhanced T1 SPACE, and DSA in grading stenosis was analyzed using Kendall's rank correlation coefficients and weighted Cohen  $\kappa$  coefficients. The values of  $\kappa$  of 0.21–0.4, 0.41–0.6, 0.61–0.8, 0.81–0.90, and 0.91–1 were considered poor, fair, moderate, good, and excellent.

A  $P$  value < 0.05 (two-tailed  $P$  value) was considered statistically significant. All calculations were performed using Microsoft Excel 2013 (Microsoft Office; Microsoft, WA, USA) and IBM SPSS Statistics for Windows version 23.0 (IBM Corp., NY, USA).

### 3. Results

#### 3.1. Summary of demographic and clinical characteristics

62 patients with clinical symptoms were enrolled (Table 1). These included 17 males and 45 females with a mean age of  $37.8 \pm 13.3$  years and mean body mass index  $25.77 \pm 3.48$  kg/m<sup>2</sup>. All patients presented with headache (61.3%,  $n = 38$ ), visual loss (33.9%,  $n = 21$ ) or pulsatile tinnitus (4.8%,  $n = 3$ ). Empty sella was identified in 27.4% ( $n = 17$ ) of the patients, posterior globe flattening was identified in 11.3% ( $n = 7$ ) of the patients, and vertical tortuosity of the optic nerve was identified in 27.4% ( $n = 17$ ) of the patients. Further, all patients underwent lumbar puncture of which 51 patients show an elevated intracranial pressure (ICP)  $\geq 200$  mmH<sub>2</sub>O, and the mean CSF opening pressure was  $311 \pm 113$  mmH<sub>2</sub>O.

#### 3.2. Angiography result

In 62 patients, 89.5% stenosis segments (111/124) at the transverse sinus was detected by DSA; 13 patients had unilateral transverse sinus stenosis, and 49 patients had bilateral transverse sinus stenosis. No immediate complications were identified after the procedure.

#### 3.3. Comparison of the two MR sequences

The sensitivity and specificity of stenosis measured with PC MRV and enhanced T1 SPACE in comparison with DSA are summarized in Table 2. For the measured stenosis, better correlation was observed in enhanced T1 SPACE and DSA (AUC = 0.953) compared with PC MRV (AUC = 0.871).

Based on the 5-grade scale, the agreement with respect to venous stenosis between the two researchers was similar for PC MRV (weighted  $\kappa = 0.813$ ) and enhanced T1 SPACE (weighted  $\kappa = 0.792$ , respectively). The consistent results of enhanced T1 SPACE, PC MRV and DSA were shown in Supplement Table 2.

The agreement for enhanced T1 SPACE ( $r_k = 0.895$ ) was better than

**Table 2**  
Performance of two MR sequences for detecting TSS compared with DSA.

	TSS	DSA		Sensitivity, % (95% CI)	Specificity, % (95% CI)	AUC (95% CI)
		Y	N			
MRV	Y	108	3	97.3 (91.7–99.3)	76.9 (46.0–93.8)	0.871
	N	3	10			
enhancedT1 SPACE	Y	109	1	98.2 (93.0–99.7)	92.3 (62.1–99.6)	0.953
	N	2	12			

TSS: transverse sinus stenosis; DSA: digital subtraction angiography; MRV: magnetic resonance venography; T1 SPACE: high-resolution variable flip angle turbo-spin-echo; CI: confidence interval.

**Table 3**  
Agreement between enhanced T1 SPACE and DSA for the grades of TSS.

enhancedT1 SPACE	DSA					Total	$r_k$	Weighted $\kappa$ (95% CI)
	0	1	2	3	4			
0	23	2	0	0	0	25	0.895	0.868 (0.811–0.926)
1	1	36	7	2	0	46		
2	0	0	25	3	0	28		
3	0	0	2	8	1	11		
4	0	0	0	2	12	14		
Total	24	38	34	15	13	124		

$r_k$ , Kendall's rank correlation coefficient; weighted  $\kappa$  using squared discrepancies. DSA: digital subtraction angiography; T1 SPACE: high-resolution variable flip angle turbo-spin-echo; CI: confidence interval.

**Table 4**  
Agreement between MRV and DSA for the grades of TSS.

MRV	DSA					Total	$r_k$	Weighted $\kappa$ (95% CI)
	0	1	2	3	4			
0	23	16	3	0	0	42	0.753	0.653 (0.565–0.740)
1	0	22	17	5	0	44		
2	1	0	12	2	0	15		
3	0	0	2	5	3	10		
4	0	0	0	3	10	13		
Total	24	38	34	15	13	124		

$r_k$ , Kendall's rank correlation coefficient; weighted  $\kappa$  using squared discrepancies. DSA: digital subtraction angiography; MRV: magnetic resonance venography; CI: confidence interval.

that for PC MRV ( $r_k = 0.753$ ) compared with DSA. For the 5-grade scale, the intermodality agreement between enhanced T1 SPACE and DSA was good (weighted  $\kappa = 0.868$ , 95% CI 0.811–0.926, Table 3). The intermodality agreement was moderate between PC MRV and DSA (weighted  $\kappa = 0.653$ , 95% CI 0.565–0.740, Table 4).

#### 3.4. Characterization of enhanced T1 SPACE

Further, 37 intrasinus filling defects were detected in 25 patients using enhanced T1 SPACE, all of these filling defects were in accordance with intrasinus filling defects on DSA, while only twenty of them were detected on source imaging of PC MRV. Also, 59.7% ( $n = 37$ ) of patients had TSS without an intrasinus filling defect, 27.4% ( $n = 17$ ) had one filling defect, 6.5% ( $n = 4$ ) had two filling defects, and 6.5% ( $n = 4$ ) had three filling defects. Moreover, 78.4% (29/37) of the filling defects were identified in transverse sinuses, 21.6% (8/37) of the filling defects were identified in junction of transverse-sigmoid sinuses. The geometric shape was funicular in 13.5% (5/37) and granular in 86.5% (32/37) of these filling defects.

### 4. Discussion

This prospective study compared the accuracy of enhanced T1 SPACE with PC MRV in detecting transverse sinus stenosis using DSA as the gold standard. The results demonstrated the superiority of enhanced T1 SPACE over PC MRV in detecting stenosis (weighted  $\kappa = 0.868$  vs 0.653). The enhanced T1 SPACE sequence could accurately detect intrasinus lesions and measure the severity of sinus stenosis, which might be useful in patient selection before catheter-based DSA imaging and provide a reference in optimizing medical therapy and guiding early invasive management, such as acetazolamide or venous sinus stenting [20,21].

In the present study, the sensitivity of enhanced T1 SPACE in depicting venous stenosis was comparable with that of PC MRV, and the

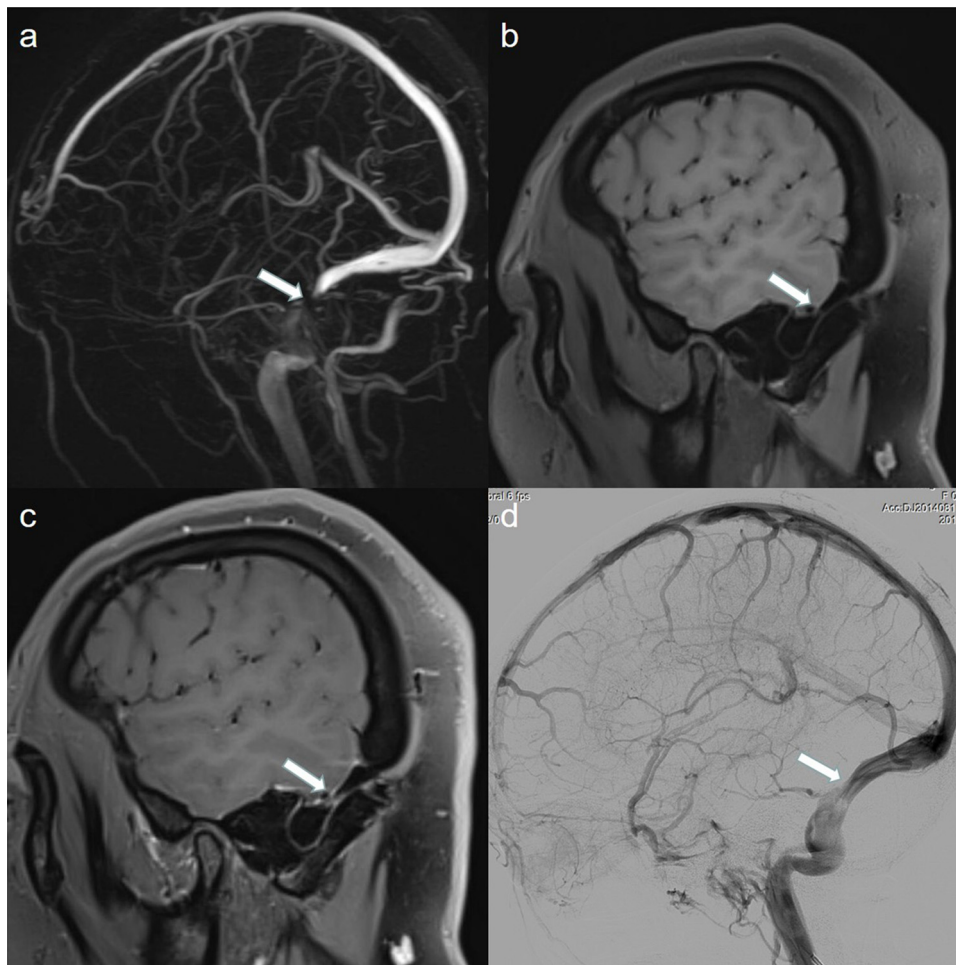


**Fig. 1.** Right distal transverse sinus stenosis in a 30-year-old female patient. The stenosis (white arrow) was shown on the sagittal view of (a) PC MRV, (b) T1 SPACE, (c) enhanced T1 SPACE, (d) DSA. The grade scale of the stenosis was 2 on DSA, 1 on T1 SPACE and enhanced T1 SPACE, but 0 on MRV.

specificity was better than that of PC MRV. Overestimation occurred in two cases of moderate stenosis because of heterogeneous signals from the lumen. The distal transverse sinus is often afflicted with stenosis. MRV imaging demonstrates the intra-sinus blood flow and is usually challenging in this location owing to the irregular geometry and complex flow patterns [22]. Consequently, measurements of the distal transverse sinus stenosis are often inaccurate. MRV cannot differentiate compression from occlusion. The speed of intra-sinus blood flow affects the signal intensity. Hence, the sinus with stenosis might be exaggerated as occlusion in case of the abnormal shape and stagnant blood flow in the transverse sinus. In the present study, nearly more than 50% patients were overestimated as grade 0 in PC MRV sequence compared with enhanced T1 SPACE sequence. The enhanced T1 SPACE technique facilitated the visualization of the wall of venous sinus by depression of the blood signal inside the sinus [22,23]. The black-blood contrast helped in reducing the false-positive diagnosis due to flow artifacts commonly observed on PC MRV, as shown in Fig. 1. The eT1 SPACE sequence demonstrated high intrinsic SNR/CNR efficiency, allowing for volume acquisitions with 0.72-mm resolution along the slice direction. The technique could depict the structure of the transverse sinus in detail, and help radiologists to achieve diagnosis with high inter-observer agreement concerning the wall invasion and lumen occlusion by para-sinus lesions, which actually made up the pitfalls of MRV [22]. This suggested that the black-blood feature was a major contributor to the high detection accuracy of TSS in this study.

Hypoplastic or aplastic transverse sinus is a common variation, and 15%–30% of the patients in previous studies had unilateral hypoplasia

or aplasia of the transverse sinus [24,25]. It might be difficult to distinguish the hypoplastic sinus from thrombosis with PC MRV alone for the absence of signal within a sinus, usually the left transverse sinus [13]. This would be more challenging when using conventional T1 SPACE in the cerebral venous system where anatomic variants, including sinus atresia/hypoplasia asymmetrical sinus drainage, are commonly present. There were higher consistency in grade 0–2 compared with DSA, which indicated that the accuracy of enhanced T1 SPACE was better than PC MRV in detecting severe sinus stenosis. Compared with PC MRV, the enhanced T1 SPACE technique could get precise imaging of insidious regions with complex flow geometry and slow flow by its excellent background suppression. In this study, a substantial improvement in imaging was observed in the artifactual regions when incorporating T1 SPACE with Gd-DTPA preparation compared with conventional T1 SPACE imaging. A significantly elevated signal contrast between these lumen regions and the surrounding vessel wall sufficed to detect the filling defects attached to the wall effectively.

Intrasinus filling defects were regarded as a reason of transverse sinus stenosis [26]. Some filling defects could be detected by enhanced T1 SPACE and DSA. These filling defects were presumed to be arachnoid granulations [27,28]. The arachnoid granules were regarded as the main source of filling defects in the sinus and the chronic thrombus as another source of filling defects. MRV sequence could only depict filling defects but cannot distinguish arachnoid granules from sinus wall. The non-enhanced T1 SPACE depicted a subacute thrombus as a hyperintense signal. But the chronic thrombus components might appear

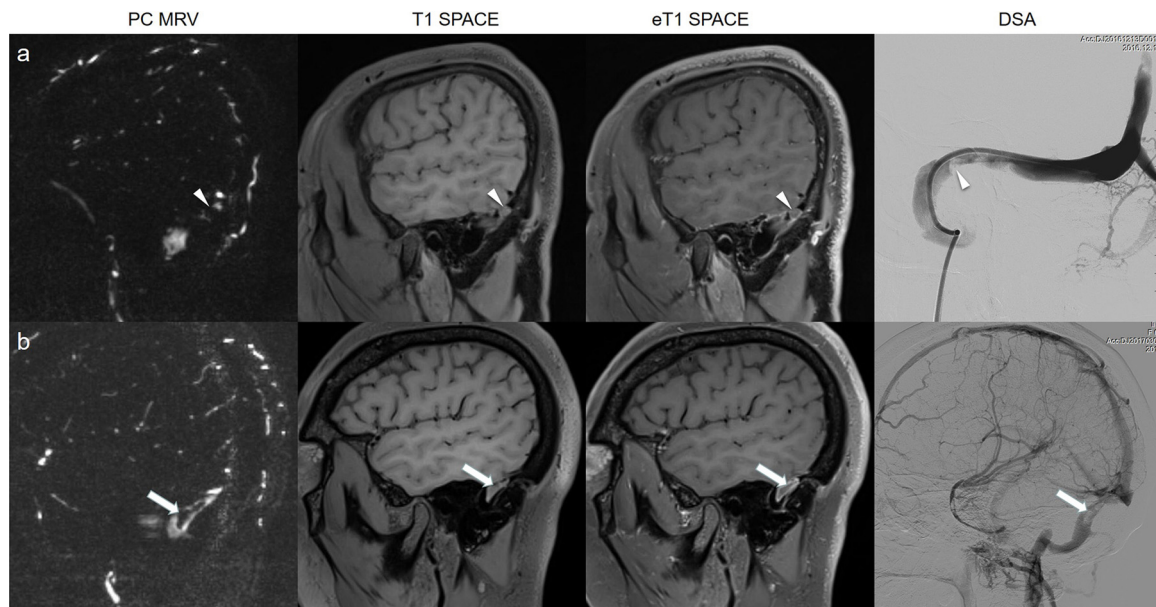


**Fig. 2.** Example of granular and funicular intrasinus filling defect. The abnormal granular signal (white arrowhead) in patient (a) was obviously different from the funicular signal (white arrow) in patient (b) using PC MRV, T1 SPACE, enhanced T1 SPACE sequences, and DSA.

isointense, which is similar to background tissues such as the blood, vessel wall, and surrounding brain tissues [16]. As a result, a part of the chronic thrombus could be mistaken as venous wall or surrounding brain tissues by non-enhanced T1 SPACE. The sinus anatomy structures, such as sinus wall, arachnoid granules, and surrounding tissues, were well visualized on enhanced T1 SPACE. It was concluded that the arachnoid granules were mostly granular with only surface enhanced. With gadolinium contrast material diffused into the intravascular thrombus [3], the chronic thrombus showed heterogeneous funicular enhancement. Five filling defects of suspected chronic thrombus were observed in this study, as shown in Fig. 2. Anticoagulant therapy might be reasonable in the following treatment for patients with an intrasinus chronic thrombus.

This study had several limitations. First, the sample was from a single center and had a relatively small size. Further studies are warranted to verify the accuracy of enhanced T1 SPACE in evaluating transverse sinus stenosis. Second, the artifacts caused by the patients' movement during examination may affect the result judgment. Third, the study had no control group of normal patients for the risk of invasive angiography; hence, the prevalence of TSS in cohorts without clinical symptoms was unclear. Fourth, follow-up imaging was absent in this study. Therefore, the relationship between the filling defect and the therapy result remained unclear.

## 5. Conclusions

Contrast-enhanced T1 SPACE is a valid noninvasive imaging technique superior to PC MRV sequence in assessing stenosis and detecting lesions in patients with TSS. Accurate determination of the presence and extent of TSS using this technique might be useful in patient selection before catheter-based DSA imaging and in guiding the following therapy.

## IRB statement

This study was approved by the institutional review board, and written informed consent was obtained from all patients.

## Declaration of Competing Interest

All authors declare that they have no conflict of financial interest.

## References

- [1] P.P. Morris, D.F. Black, J. Port, et al., Transverse sinus stenosis is the most sensitive MR imaging correlate of idiopathic intracranial hypertension, *AJNR Am. J. Neuroradiol.* 38 (3) (2017) 471–477.
- [2] M.B. Avery, S. Sambrano, E.J. Khader, et al., Accuracy and precision of venous pressure measurements of endovascular microcatheters in the setting of dural venous sinus stenosis, *J. Neurointerv. Surg.* (2017).
- [3] A.M. Saindane, B.C. Mitchell, J. Kang, et al., Performance of spin-echo and gradient-echo T1-weighted sequences for evaluation of dural venous sinus thrombosis and stenosis, *AJR Am. J. Roentgenol.* 201 (1) (2013) 162–169.
- [4] L.P. Kelly, A.M. Saindane, B.B. Bruce, et al., Does bilateral transverse cerebral venous sinus stenosis exist in patients without increased intracranial pressure? *Clin. Neurol. Neurosurg.* 115 (8) (2013) 1215–1219.
- [5] G.A. Bateman, Arterial inflow and venous outflow in idiopathic intracranial hypertension associated with venous outflow stenoses, *J. Clin. Neurosci.* 15 (4) (2008) 402–408.
- [6] R.I. Farb, I. Vanek, J.N. Scott, et al., Idiopathic intracranial hypertension: the prevalence and morphology of sinovenous stenosis, *Neurology* 60 (9) (2003) 1418–1424.
- [7] J.A. Lansley, W. Tucker, M.R. Eriksen, et al., Sigmoid sinus diverticulum, Dehiscence, and venous sinus stenosis: potential causes of pulsatile tinnitus in patients with idiopathic intracranial hypertension? *AJNR Am. J. Neuroradiol.* 38 (9) (2017) 1783–1788.
- [8] D. Gandhi, Computed tomography and magnetic resonance angiography in cervicocranial vascular disease, *J. Neuroophthalmol.* 24 (4) (2004) 306–314.
- [9] J.N. Higgins, J.H. Gillard, B.K. Owler, et al., MR venography in idiopathic intracranial hypertension: unappreciated and misunderstood, *J. Neurol. Neurosurg. Psychiatry* 75 (4) (2004) 621–625.
- [10] R.I. Farb, J.N. Scott, R.A. Willinsky, et al., Intracranial venous system: gadolinium-enhanced three-dimensional MR venography with auto-triggered elliptic centric-ordered sequence—initial experience, *Radiology* 226 (1) (2003) 203–209.
- [11] F. Fera, F. Bono, D. Messina, et al., Comparison of different MR venography techniques for detecting transverse sinus stenosis in idiopathic intracranial hypertension [J], *J. Neurol.* 252 (9) (2005) 1021–1025.
- [12] M. Wall, Idiopathic intracranial hypertension, *Neurol. Clin.* 28 (3) (2010) 593–617.
- [13] L. Liang, Y. Korogi, T. Sugahara, et al., Evaluation of the intracranial dural sinuses with a 3D contrast-enhanced MP-RAGE sequence: prospective comparison with 2D-TOF MR venography and digital subtraction angiography, *AJNR Am. J. Neuroradiol.* 22 (3) (2001) 481–492.
- [14] J.L. Leach, M. Wolujewicz, W.M. Strub, Partially recanalized chronic dural sinus thrombosis: findings on MR imaging, time-of-flight MR venography, and contrast-enhanced MR venography, *AJNR Am. J. Neuroradiol.* 28 (4) (2007) 782–789.
- [15] B. Jeevanandham, T. Kalyanpur, P. Gupta, et al., Comparison of post-contrast 3D-T1-MPRAGE, 3D-T1-SPACE and 3D-T2-FLAIR MR images in evaluation of meningeal abnormalities at 3-T MRI, *Br. J. Radiol.* 90 (1074) (2017) 20160834.
- [16] Q. Yang, J. Duan, Z. Fan, et al., Early detection and quantification of cerebral

- venous thrombosis by magnetic resonance black-blood Thrombus imaging, *Stroke* 47 (2) (2016) 404–409.
- [17] P.P. Niu, Y. Yu, Z.N. Guo, et al., Diagnosis of non-acute cerebral venous thrombosis with 3D T1-weighted black blood sequence at 3T, *J. Neurol. Sci.* 367 (2016) 46–50.
- [18] P.J. Maralani, M. Hassanlou, C. Torres, et al., Accuracy of brain imaging in the diagnosis of idiopathic intracranial hypertension, *Clin. Radiol.* 67 (7) (2012) 656–663.
- [19] S. Bidot, A.M. Saindane, J.H. Peragallo, et al., Brain imaging in idiopathic intracranial hypertension, *J. Neuroophthalmol.* 35 (4) (2015) 400–411.
- [20] K.A. Markey, S.P. Mollan, R.H. Jensen, et al., Understanding idiopathic intracranial hypertension: mechanisms, management, and future directions, *Lancet Neurol.* 15 (1) (2016) 78–91.
- [21] H. Saber, W. Lewis, M. Sadeghi, et al., Stent survival and stent-adjacent stenosis rates following venous sinus stenting for idiopathic intracranial hypertension: a systematic review and meta-analysis, *Interv. Neurol.* 7 (6) (2018) 490–500.
- [22] D. Wang, Y. Lu, B. Yin, et al., 3D fast spin-echo T1 black-blood imaging for the preoperative detection of venous sinus invasion by meningioma : comparison with contrast-enhanced MRV, *Clin. Neuroradiol.* (2017).
- [23] Y. Qiao, D.A. Steinman, Q. Qin, et al., Intracranial arterial wall imaging using three-dimensional high isotropic resolution black blood MRI at 3.0 Tesla, *J. Magn. Reson. Imaging* 34 (1) (2011) 22–30.
- [24] R.H. Ayanzen, C.R. Bird, P.J. Keller, et al., Cerebral MR venography: normal anatomy and potential diagnostic pitfalls, *AJNR Am. J. Neuroradiol.* 21 (1) (2000) 74–78.
- [25] J. Wang, J. Wang, J. Sun, et al., Evaluation of the anatomy and variants of internal cerebral veins with phase-sensitive MR imaging, *Surg. Radiol. Anat.* 32 (7) (2010) 669–674.
- [26] A. Donnet, P. Metellus, O. Levrier, et al., Endovascular treatment of idiopathic intracranial hypertension: clinical and radiologic outcome of 10 consecutive patients, *Neurology* 70 (8) (2008) 641–647.
- [27] L. Liang, Y. Korogi, T. Sugahara, et al., Normal structures in the intracranial dural sinuses: delineation with 3D contrast-enhanced magnetization prepared rapid acquisition gradient-echo imaging sequence, *AJNR Am. J. Neuroradiol.* 23 (10) (2002) 1739–1746.
- [28] G.V. Watane, B. Patel, D. Brown, et al., The significance of arachnoid granulation in patients with idiopathic intracranial hypertension, *J. Comput. Assist. Tomogr.* 42 (2) (2018) 282–285.